RECOVERING CRITICAL STRESSES IN SANDWICHES USING THROUGH-THETHICKNESS REINFORCEMENT

RECOVERING CRITICAL STRESSES IN SANDWICHES USING THROUGH-THE-THICKNESS REINFORCEMENT

ICARDI U. °, SOLA F.

Dipartimento di Ingegneria Meccanica e Aerospaziale

Politecnico di Torino - Corso Duca degli Abruzzi 24, 10129 Torino, Italy

° Corresponding author. Tel: +39 (0)115646872; fax: +39 (0)115646899

E-mail addresses: ugo.icardi@polito.it (U. Icardi); fedrico.sola@polito.it (F. Sola)

Abstract

The paper is aimed at investigating the effects of stitching or tufting on displacement and stress fields of sandwiches, whose homogenized mechanical properties are computed through virtual material tests with 3D finite element analysis. After that, structural analysis is carried out using the adaptive model by the authors, which has variable representation of displacements across the thickness and fixed degrees of freedom. This choice is done considering its accuracy and computational efficiency. Numerical applications show that using these technical skills it is possible to considerably reduce stresses and displacements in sandwiches.

Keywords: A. Fabrics/ textile; **B.** Stress relaxation; **C.** Analytical modelling; **C.** Finite element analysis;

1 Introduction

Composites find use as primary structural components in aerospace and other branches of engineering, because they ranked high in stiffness and strength. Sandwiches with laminated faces are widespread in lightweight design thanks to an outstanding specific stiffness compared to monolithic composite structures (see e.g. Heimbs et al. [1]). Regrettably, composites suffer from strong stress concentrations at the interfaces, which can have harmful effects on structural performance and service life, as exhaustively explained among many others in the works by De Borst and Remmers [2], Davies et al. [3] and Ajdari et al. [4].

Many technical skills have been developed with the aim of overcoming this problem. As far as laminates are concerned, stitching is largely employed. Gui and Li [5] demonstrated that this technique can improve the buckling behaviour, while Mouritz [6] showed that the fracture toughness of stitched laminates is much higher than the equivalent unstitched ones. Shah Khan and Mouritz [7] reported that the

translaminar strength of fibre reinforced polymer (FRP) composites can be improved considerably with a thread of carbon, glass or Kevlar.

Many approaches have been suggested for sandwiches: folded core (Heimbs et al. [1]), stitching of faces and stitching through-the-thickness (Potluri et al. [8]), integrated pile core (Judawisastra et al. [9]) and vertical composite columns, 3D pins or shear keys implanted in the core (Wang et al. [10], Vaidya et al. [11] and Nilanjan [12]). These techniques have been proven successful in improving the performance of sandwiches under impact loading (Heimbs et al. [1], Potluri et al. [8] and Vaidya et al. [11]), the fatigue behaviour (Judawisastra et al. [9]) and the shear properties (Wang et al. [10] and Nilanjan [12]). However the Advanced Composites Technology (ACT) program proposed by NASA [13] demonstrated that stitching through-the-thickness is the most effective technical skill in reducing costs and improving damage tolerance of aircraft structures. The stitching procedure requires the insertion of reinforcement in the through-the-thickness direction of the structure. It could be noticed that this technique is easy to use with the current manufacturing technologies and that stitching is mostly employed with dry fabric preforms, since the tackiness of the uncured resin makes sewing difficult in uncured pre-preg laminate. Another available technique, which inserts reinforcement in the through-the-thickness direction, is tufting. This procedure uses a single needle instead of a dual threading system. In this way the thread is introduced into the structures without tension, thus avoiding any detrimental effects on the mechanical performance of the 3D fibre architecture, as outlined in [14].

The insertion of a through-the-thickness reinforcement introduces the idea of 3D material. Within this framework, several approaches, validated by comparisons with experimental results or 3D FEA, have been suggested for modelling the mechanical behaviour of this kind of materials. According to Prodromou et al. [15], they can be broadly classified into four classes, here referred as: i) analytical methods, ii) methods based upon inclusion method, iii) methods based upon cell method and iv) FEM methods. The analytical methods (see, e.g. [16–18]) are based on laminate theory and orientation averaging techniques. In these models, the composite is discretized into small volume elements, which can be treated as a unidirectional lamina with transverse isotropic properties. Making the assumption of either iso-stress, or iso-strain, the macroscopic properties are determined by volume averaging the response of a composite representative body. These methods give an accurate prediction for in-plane on-axis moduli, while shear and out-of-plane properties could be predicted with significant errors, as outlined

in [15] and [19]. Inclusion methods [20, 21] adopt a mean field approach based upon the equivalent inclusion theory [22], for evaluating the mechanical properties. However, comparisons with experiments showed that average errors relative to experimental results of at least 10 % can be found with this technique, as reported in [15].The cell method [15, 23] is based on the theory of continuum media. It firstly split the structure into representative volume elements, which repeat itself throughout the material. The following step requires defining the macroscopic average stresses and strains from the microscopic ones, next continuity of traction and displacements should be imposed at the interfaces between the constituent volumes. In the final step the overall elasto-plastic behaviour is determined by expressing it as a constitutive relationship between the average stress, strain and plastic strain, in conjunction with the effective elastic stiffness tensor of the composite. With respect to the inclusion methods, it is possible to halve the average errors relative to experimental results, as shown in [15]. According to [15], the most accurate approach to date available is that based on material testing carried out with full scale finite element analysis (FEA), as proposed in [24] and [25]. This approach is also the most computationally expensive, since a complex finite element 3D model is required.

The aim of this paper is to show that the insertion of a through-the-thickness reinforcement considerably reduces interlaminar stresses at critical interfaces, thus giving a possible explanation of the experimental results shown in literature dealing with the reduction of damage in sandwiches undergoing impact loading (e.g. [8] and [14]). For doing this, we choose to carry out virtual material tests using the 3D finite element [26], in order to get an evaluation of the homogenized mechanical properties of stitched or tufted sandwiches. Then we carry out the structural analysis using the adaptive model [29]. In this way, costs are affordable, as 3D FEA is required only once for any specific case, while, thanks to its efficiency, the adaptive model consistently speeds-up the structural analysis.

It could be noticed that the use of techniques, which suppose a repetitive scheme in the material structure, cannot be always satisfactory since their basic assumption could be violated. For instance, methods based on repetitive schemes could be unsuited to simulate localized damages that are not spread throughout all the structure, such as core's crushing, which strongly affects damage formation (see, e.g. [27] and [28]). The adaptive model [29] has a fixed number of functional degrees of freedom (d.o.f.), which are the same of classical plate models: the three mid-plane displacements and the two shear rotations. As a consequence, it is advantageous when a large number of iteration are required for computing the

structural response, like under impact loading (see, e.g. [1, 8]). The structural model is derived from that developed in [33], in order to preserve accuracy and considerably improve efficiency through a reduced processing time, as discussed forward.

This model can be set among the high order layerwise (HLW) models, which are, at the present, adopted by many researchers (see e.g. [30], [31] and [32]), because they obtain refined estimates like 3-D models but with a much lower number of unknowns. The distinctive feature of HLW models is whether their number of functional d.o.f. depends or not on the number of physical or computational layers. In the former case computational costs rise increasing the number of layers, while in the latter the number of unknowns is fixed.

The paper is structured as follows. First of all the basic steps for developing of the adaptive model by the authors are reviewed. Then, the method adopted for evaluating the homogenized mechanical properties of stitched or tufted sandwiches is described. Next, applications are presented, first of all, in order to assess whether the adaptive model can be employed for the analysis of textile composites and to assess the accuracy of the strategy adopted for modelling the through-the-thickness reinforcement. Finally, applications are presented to show the effects of stitching or tufting on stress and displacement fields of sandwich plates and beams.

2 The adaptive model

In this paper we use the model [29], whose most important merit with respect is overcoming of the drawbacks related to the algebraic computations, required to evaluate coefficients of higher-order terms and continuity functions of model [33]. The displacement field of the present model is similar to that presented in [33], but it is much more efficient since continuity functions and high-order terms are calculated apart in closed form once at a time, as explained forward. This consistently speeds-up computation of solutions as it allows reducing of up 20 times the computational effort with respect to the model [33]. In details, on a laptop computer with a 1800 GHz double-core processor and 2,96 GB RAM the analysis of a simply supported sandwich beam requires 1,35 sec using the present model, while it requires 22,5 sec using the model [33].

The present model is characterized by a variable representation from point to point across the thickness, with the aim to always accurately predict the stress field directly from constitutive equations, either for laminates or sandwiches ([30], [31] and [32]). In fact, the order of polynomials cannot be the same for

any point across the thickness, and in addition it should vary according to the type of loading, the boundary conditions, the thickness ratio and the constituent materials. Since the present model has the same five d.o.f. of equivalent single layer models, its processing time is minimal, thus it can be successfully applied to highly iterative analyses, like transient dynamics and non-linear analyses. This motivates our choice of the structural model. The displacement field is assumed as follows [29]:

$$u(x,y,z) = u^0(x,y) + z(\gamma_x^0(x,y) - w^0{}_{,x}) + C_x^i(x,y)z^2 + D_x^i(x,y)z^3 + (Oz^4...) + \sum_{k=1}^{n_i}\Phi_x^k(x,y)(z-z_k)H_k + \sum_{k=1}^{n_i}C_u^k(x,y)H_k \quad (1)$$

$$v(x,y,z) = v^0(x,y) + z(\gamma_y^0(x,y) - w^0{}_{,y}) + C_y^i(x,y)z^2 + D_y^i(x,y)z^3 + (Oz^4...) + \sum_{k=1}^{n_i}\Phi_y^k(x,y)(z-z_k)H_k + \sum_{k=1}^{n_i}C_v^k(x,y)H_k \quad (2)$$

$$w(x,y,z) = w^0(x,y) + b^i(x,y)z + c^i(x,y)z^2 + d^i(x,y)z^3 + e^i(x,y)z^4 + (Oz^5...) + \sum_{k=1}^{n_i}\Psi^k(x,y)(z-z_k)H_k + \\ + \sum_{k=1}^{n_i}\Omega^k(x,y)(z-z_k)^2H_k + \sum_{k=1}^{n_i}C_w^k(x,y)H_k \quad (3)$$

The superscripts i mean that these terms are valid only in a specific range across the thickness, thus enabling different representation from point to point. This aspect together with the addition of the continuity functions C_u^k, C_v^k and C_w^k represents the new contributions with respect to the model [33], where just the higher-order terms were assumed to vary with position. Please note that H_k is the unit step function.

Like for classical models, the functional d.o.f. still remain 5: the three displacements u^0, v^0, w^0 and the two shear rotations γ_x^0, γ_y^0 of the points on the reference middle surface of the plate. Refinement of the solution can be obtained by an appropriate choice of the contributions $(Oz^4...)$ and $(Oz^5...)$ or by increasing the number of subdivisions across the thickness, in both cases avoiding a growth in the number of primary variables.

The purpose of the terms in the summations, i.e. the zig-zag contributions, is to make discontinuous the derivatives of displacements at the layer interfaces. In this way it is possible to fulfil *a priori* the constraints prescribed by the elasticity theory:

$$\sigma_{xz}(z={}^{(k)}z^+) = \sigma_{xz}(z={}^{(k+1)}z^-) \quad \sigma_{yz}(z={}^{(k)}z^+) = \sigma_{yz}(z={}^{(k+1)}z^-) \quad \sigma_z(z={}^{(k)}z^+) = \sigma_z(z={}^{(k+1)}z^-) \quad \sigma_{z,z}(z={}^{(k)}z^+) = \sigma_{z,z}(z={}^{(k+1)}z^-) \quad (4)$$

$$u(z={}^{(k)}z^+) = u(z={}^{(k+1)}z^-) \quad v(z={}^{(k)}z^+) = v(z={}^{(k+1)}z^-) \quad w(z={}^{(k)}z^+) = w(z={}^{(k+1)}z^-) \quad (5)$$

The coefficients C_x^i, C_y^i, D_x^i, D_y^i, as well as the other high order terms are determined by enforcing the boundary conditions for transverse shear stresses, transverse normal stress and its gradient at the upper and lower bounding surfaces:

$$\sigma_{xz}|^u = 0 \quad \sigma_{xz}|_l = 0 \quad \sigma_{yz}|^u = 0 \quad \sigma_{yz}|_l = 0 \quad \sigma_z|^u = p^0|^u \quad \sigma_z|_l = p^0|_l \quad \sigma_{z,z}|^u = 0 \quad \sigma_{z,z}|_l = 0 \tag{6}$$

(p^0 represents the transverse distributed loading).

In addition also the equilibrium condition at discrete points across the thickness should be enforced:

$$\sigma_{x,x} + \sigma_{xy,y} + \sigma_{xz,z} = 0 \quad \sigma_{xy,x} + \sigma_{y,y} + \sigma_{yz,z} = 0 \quad \sigma_{xz,x} + \sigma_{yz,y} + \sigma_{z,z} = 0 \tag{7}$$

The constraint of Eq. (7) should be imposed in $n_p = N_{lay} \cdot ord\_u - 2$ points across the thickness, where N_{lay} is the number of computational layers, while *ord_u* is the order of the expansion chosen for the in-plane displacements. The n_p points are chosen trying to fulfil the equilibrium condition (7) in all the points across the thickness of the structure. The n_p points should not be placed excessively near to the layers' interfaces, in order to avoid singularity.

In order to get the expressions of all the unknowns (i.e. continuity functions and hierarchic terms), the displacements are split into fixed contributes, layer's contributes and summations' contributes, as follows:

$$u(x,y,z) = U^0(x,y,z) + U^i(x,y,z) + \sum_{k=1}^{n_i} \Phi_x^k(x,y)(z-z_k)H_k + \sum_{k=1}^{n_i} C_u^k(x,y)H_k \tag{8}$$

$$v(x,y,z) = V^0(x,y,z) + V^i(x,y,z) + \sum_{k=1}^{n_i} \Phi_y^k(x,y)(z-z_k)H_k + \sum_{k=1}^{n_i} C_v^k(x,y)H_k \tag{9}$$

$$w(x,y,z) = W^0(x,y,z) + W^i(x,y,z) + \sum_{k=1}^{n_i} \Psi^k(x,y)(z-z_k)H_k + \sum_{k=1}^{n_i} \Omega^k(x,y)(z-z_k)^2 H_k + \sum_{k=1}^{n_i} C_w^k(x,y)H_k \tag{10}$$

The expressions of the displacement continuity functions C_u^k, C_v^k and C_w^k at a generic interface $\Im$ are obtained enforcing Eq. (5):

$$C_u^k(x,y) = U^i(x,y,z_\Im) - U^{i+1}(x,y,z_\Im) \quad C_v^k(x,y) = V^i(x,y,z_\Im) - V^{i+1}(x,y,z_\Im) \quad C_w^k(x,y) = W^i(x,y,z_\Im) - W^{i+1}(x,y,z_\Im) \tag{11}$$

As example, the explicit form of Eq. (4) for a beam at the generic interface $\Im$ between the layers *i* and *i+1* is reported:

$$\Phi_x^\Im = \frac{Q_{44}^-}{Q_{44}^+}\left(U_{,z}^{\,i} + W_{,x}^{\,i}\right) - U_{,z}^{\,i+1} - W_{,x}^{\,i+1} - C_{w,x}^\Im + \frac{\left(Q_{44}^- - Q_{44}^+\right)}{Q_{44}^+}\left(U_{,z}^{\,0} + \sum_{k=1}^{q-1}\Phi_x^k + W_{,x}^{\,0} + \sum_{k=1}^{q-1}\Psi_{,x}^{\,k}\left(z_\Im - z_k\right) + \sum_{k=1}^{q-1}\Omega_{,x}^{\,k}\left(z_\Im - z_k\right)^2 + \sum_{k=1}^{q-1} C_{w,x}^k\right) \tag{12}$$

$$\Psi^\Im = \frac{Q_{13}^-}{Q_{33}^+}U_{,x}^{\,i} + \frac{Q_{33}^-}{Q_{33}^+}W_{,z}^{\,i} - \frac{Q_{13}^+}{Q_{33}^+}\left(U_{,x}^{\,i+1} + C_{u,x}^\Im\right) - W_{,z}^{\,i+1} + \frac{\left(Q_{33}^- - Q_{33}^+\right)}{Q_{33}^+}\left(\sum_{k=1}^{q-1}\Psi^k + 2\sum_{k=1}^{q-1}\Omega^k\left(z_\Im - z_k\right)\right) + \frac{\left(Q_{13}^- - Q_{13}^+\right)}{Q_{33}^+}\left(U_{,x}^{\,0} + \sum_{k=1}^{q-1}\Phi_{,x}^{\,k}\left(z_\Im - z_k\right) + \sum_{k=1}^{q-1} C_{u,x}^k\right) \tag{13}$$

$$\Omega^{\Im}=\frac{Q_{13}^{-}}{2Q_{33}^{+}}U,_{xz}^{i}+\frac{Q_{33}^{-}}{2Q_{33}^{+}}W,_{zz}^{i}-\frac{Q_{13}^{+}}{2Q_{33}^{+}}\left(U,_{xz}^{i+1}+\Phi_{x}^{\Im},_{x}\right)-\frac{W,_{zz}^{i+1}}{2}+\frac{\left(Q_{33}^{-}-Q_{33}^{+}\right)}{Q_{33}^{+}}\sum_{k=1}^{q-1}\Omega^{k}+\frac{\left(Q_{13}^{-}-Q_{13}^{+}\right)}{2Q_{33}^{+}}\left(U,_{xz}^{0}+\sum_{k=1}^{q-1}\Phi_{x}^{k},_{x}\right) \quad (14)$$

From Eqs. (12) – (14) the expressions of the stress continuity functions are obtained. The procedure for plates is similar but it is here omitted for sake of brevity. The high order terms in Eqs. (1) - (3) are obtained by solving (7), whose explicit form for the evaluation of the generic higher order terms of a beam at the point z_p is:

$$Q_{11}U,_{xx}^{i}+Q_{44}U,_{zz}^{i}+\left(Q_{13}+Q_{44}\right)W,_{xz}^{i}=-Q_{11}\left(U,_{xx}^{0}+\sum_{k=1}^{q}\Phi,_{xx}^{k}\left(z_p-z_k\right)+\sum_{k=1}^{q}C_u,_{xx}^{k}\right)-\left(Q_{13}+Q_{44}\right)\left(\sum_{k=1}^{q}\Psi,_{x}^{k}+2\sum_{k=1}^{q}\Omega,_{x}^{k}\left(z_p-z_k\right)\right)-Q_{44}U,_{zz}^{0} \quad (15)$$

$$Q_{44}\left(U,_{zz}^{i}+W,_{xz}^{i}\right)+Q_{13}U,_{xz}^{i}+Q_{33}W,_{zz}^{i}=-Q_{44}\left(U,_{zz}^{0}+\sum_{k=1}^{q}\Psi,_{x}^{k}+2\sum_{k=1}^{q}\Omega,_{x}^{k}\left(z_p-z_k\right)\right)-Q_{13}\left(U,_{xz}^{0}+\sum_{k=1}^{q}\Phi_{x},_{x}^{k}\right)-2Q_{33}\sum_{k=1}^{q}\Omega^{k} \quad (16)$$

The solving system for plates is similar and it is here omitted being much lengthier.

3 Numerical applications

The goal is to show the effects of through-the-thickness reinforcement on stress and displacement fields of sandwiches. All the cases presented consider simply supported structures undergoing sinusoidal loading. This scheme is chosen because it is the only one for which exact elasticity solutions can be calculated and used for comparisons. As a consequence, it is customary chosen by researchers (see, e.g. [30], [34] and [35]) to validate their results. In order to respect the imposed constraints, the variation of the functional d.o.f. is assumed as a trigonometric series expansion:

$$u^{0}(x,y)=\sum_{m=1}^{M}\sum_{n=1}^{N}A_{mn}\cos\left(\frac{m\pi}{L_x}x\right)\sin\left(\frac{n\pi}{L_y}y\right) \quad (17)$$

$$v^{0}(x,y)=\sum_{m=1}^{M}\sum_{n=1}^{N}B_{mn}\sin\left(\frac{m\pi}{L_x}x\right)\cos\left(\frac{n\pi}{L_y}y\right) \quad (18)$$

$$w^{0}(x,y)=\sum_{m=1}^{M}\sum_{n=1}^{N}C_{mn}\sin\left(\frac{m\pi}{L_x}x\right)\sin\left(\frac{n\pi}{L_y}y\right) \quad (19)$$

$$\gamma_{x}{}^{0}(x,y)=\sum_{m=1}^{M}\sum_{n=1}^{N}D_{mn}\cos\left(\frac{m\pi}{L_x}x\right)\sin\left(\frac{n\pi}{L_y}y\right) \quad (20)$$

$$\gamma_{y}{}^{0}(x,y)=\sum_{m=1}^{M}\sum_{n=1}^{N}E_{mn}\sin\left(\frac{m\pi}{L_x}x\right)\cos\left(\frac{n\pi}{L_y}y\right) \quad (21)$$

The Rayleigh-Ritz method is used for solving.

3.1 Evaluation of the mechanical properties through 3D FEA

Virtual material tests are carried out using the mixed solid element developed in Ref. [26], in order to compute the elastic coefficients that will be used by the adaptive model of Section 2.

The first step is creating the geometrical model of the structure, (Figures 1a and 1b). Please note that sandwiches are here treated as multilayered structures made of an arbitrary number of thin layers

constituting the faces and of a thick intermediate layer constituting the honeycomb core, whose properties are computed from the cellular properties, according to Gibson and Ashby [36]. Note that the reinforcement is modelled as an isotropic material.

Once the geometrical model is created, the elastic coefficients of the structure are computed carrying out the analysis with the 3D FE model [26]. Its nodal d.o.f. are the three displacements and the three interlaminar stresses to meet the stress and displacements continuity requirements at the interfaces. The reason for this choice is that the computational effort required is not larger than that for displacement-based counterpart solid elements, while accuracy and convergence are dramatically improved.

The in-plane moduli are evaluated with the loading scheme of Figure 1c. Using stresses and strains computed with the FEA and the constitutive equation $\{\sigma\}=[C]\{\varepsilon\}$, the homogenized elastic properties are computed in a straightforward way.

The loading scheme of Figure 1d is employed to compute the transverse modulus E_3, while that of Figure 1e is adopted to obtain the shear moduli G_{13} and G_{23}. It could be noticed that through other loading conditions all the homogenized macromechanical coefficients of [C] are evaluated.

The procedure explained is carried out using a specific value of the stitching spacing, but, as outlined in [8], this parameter plays a fundamental role in varying the stiffness of the structure. Accordingly, this effect is taken into consideration employing the rule of mixture proposed by Mori and Tanaka [20]:

$$E_{i\,f}=E_{i\,st}+k\cdot V\left(E_{1b}-E_{i\,st}\right)\ \text{(i=1,2,3)};\quad \upsilon_{ij\,f}=\upsilon_{ij\,st}+k\cdot V\left(\upsilon_{12b}-\upsilon_{ij\,st}\right);\quad G_{ij\,f}=G_{ij\,st}+k\cdot V\left(G_{12b}-G_{ij\,st}\right)\ \text{(ij=12,13,23)} \tag{22}$$

The subscripts “f”, “st” and “b” refer respectively to the stitched or tufted layer, to the standard layer and to the binder. The symbol “V” corresponds to the reinforcement percentage volume in the considered layer, thus V allows to account for the effects of the stitching spacing. Finally “k” is an index that enables to vary the mechanical properties of the material constituting the binder. Please note that the relation of Eq. (22) represents a conservative approach with respect to the effective correlation between elastic coefficients and stitching spacing, as shown in [39]. It could be remarked that no more than 60 seconds on a laptop computers are required to carry out each analysis.

As shown in Tables 1 and 2 present 3D finite element model obtains an evaluation of the mechanical properties in a very good agreement with experimental and numerical reference results.

3.2 Validation of the models

In this section first of all the mechanical properties of two stitched composites considered in literature are computed via 3D FEA using the method proposed in Section 3.1, in order to verify its accuracy. These two cases are chosen because their mechanical properties have been evaluated from experiments. Then a 3D woven composite (3DWC) is considered with the aim to assess whether the adaptive model can be successfully employed for studying textile composites.

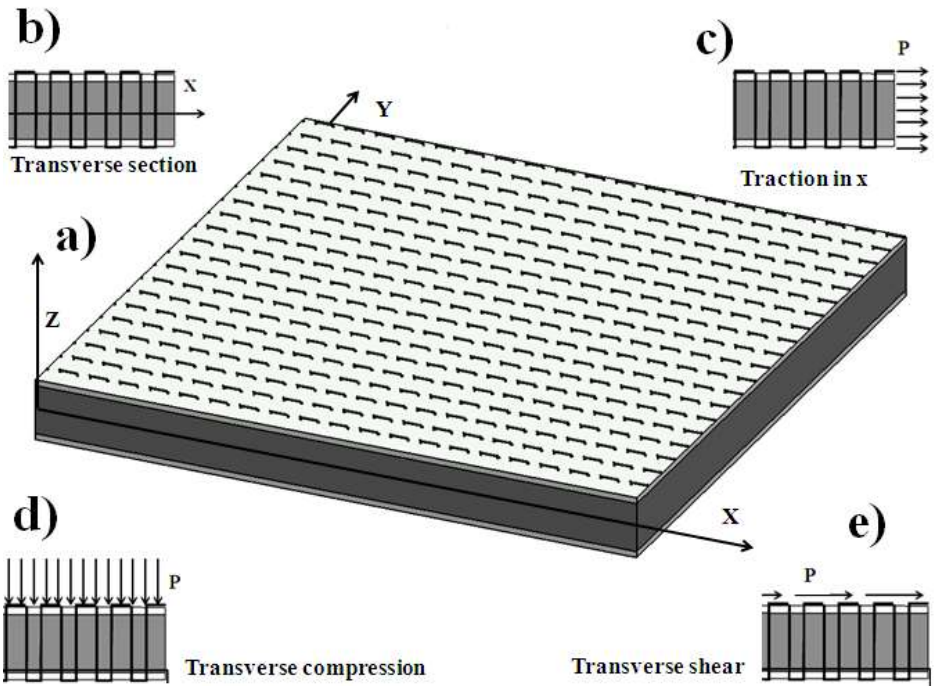

Figure 1. a) 3D model of stitched sandwich. b) Transverse section. Loading scheme for calculating c) in-plane moduli, d) transverse modulus and e) shear moduli with 3D FEA.

Table 1. Comparison between the mechanical properties calculated by Yudhanto et al. [37] and the present ones.

	Stitch pitch (mm)	6	3
E_x (MPa)	Experiment [37]	51,1 ± 1,9	51,7 ± 3,1
	Present	52,2	52,7
υ_{xy} (MPa)	Experiment [37]	0,314 ± 0,013	0,324 ± 0,005
	Present	0,317	0,325

Table 2. Comparison between the mechanical properties calculated by Lascoup et al. [38] and the present ones.

Stitching step= 12,5 mm			
		α=45°	
E_z (MPa)	Experiment [38]	206,7 ± 13,3	
	Analytical [38]	208,1	
	Present	207,5	
G_{xz} (MPa)	Experiment [38]	28,0 ± 2,1	
	Analytical [38]	42,1	
	Present	26,4	
Stitching step= 25 mm			
		α=45°	α=60°
E_z (MPa)	Experiment [38]	95,5 ± 2,1	133,5 ± 9,9
	Analytical [38]	93,9	149,3
	Present	96,1	134,1
G_{xz} (MPa)	Experiment [38]	19,4 ± 2,3	14,8 ± 1,7
	Analytical [38]	21,9	13,4
	Present	20,1	15,4
Stitching step= 50 mm			
		α=45°	
E_z (MPa)	Experiment [38]	57,9 ± 4,8	
	Analytical [38]	36,9	
	Present	59,9	
G_{xz} (MPa)	Experiment [38]	15,9 ± 0,7	
	Analytical [38]	10,9	
	Present	16,2	

As first case, let us consider the stitched laminate analysed by Yudhanto et al. in [37], who proposed experimental evaluations of the in plane moduli for a T800SC-24kf dry preforms with tow orientation of $[+45°/90°/-45°/0_2/+45°/90°_2/-45°/0]_s$, stitched with a 200 denier Vectran® thread. The preform is impregnated with epoxy resin XNR/H6813. Table 1 reports comparisons between the experimental results and the coefficients computed using the method explained in Section 3.1. From these numerical results it could be noticed that virtual material tests provide results in good agreement with experiments.

For a further assessment, we consider the sandwich studied by Lascoup et al. in [38]. This paper presents experimental results for a sandwich with a 20 mm polyurethane foam core and 1 mm E-glass fibre faces. Different configuration are analysed by varying the stitching spacing (i.e. three values of the stitching step in the X direction are considered) and the angle between through-the-thickness reinforcement and faces (here indicated with α). The reinforcing thread is made of 2400 TEX glass fibre (E=13,7 GPa) and its diameter is 2,7 mm. The stitching step in the Y direction is fixed and its value is 24 mm. Accordingly to the behaviour shown in [8], reducing the stitching spacing has a significant bearing in increasing transverse and shear modulus. From Table 1, it could be noticed that virtual material tests provide results

included in the natural dispersion of experiments, therefore the accuracy of the method proposed in Section 3.1 can be considered satisfactory.

Now we want to verify whether the structural model [29] can be successfully employed for studying textile composites, after having obtained an evaluation of the homogenized mechanical properties with 3D FEA or any another suitable technique. To this purpose let us consider the case presented in Bogdanovich and Pastore in [35], where the stress field of a 3DWC is computed using homogenized mechanical properties, whose values are explicitly provided by the authors. In details, Bogdanovich and Pastore compare three different methods, namely: case a) considers totally homogenized material, while cases b) and c) consider artificial division into three and four layers. In [35], all the elements of the 6-by-6 stiffness matrix for the three cases are specified. Thus they can be employed by the adaptive model [29] to compute the stress field. A square plate characterized by a length to thickness ratio of 10 is considered. According to [35] the stresses are reported in the following normalised form:

$$\overline{\sigma}_x = \frac{\sigma_x\left(\frac{L_x}{2}, \frac{L_y}{2}, z\right)}{p^0} \quad \overline{\sigma}_{xz} = \frac{\sigma_z\left(0, \frac{L_y}{2}, z\right)}{p^0} \tag{23}$$

where p^0 is the maximum intensity of the distributed loading. Figure 2a represents the through-the-thickness variation of the in-plane stress $\overline{\sigma}_x$ while Figure 2b represents the through-the-thickness variation of the transverse shear stress $\overline{\sigma}_{xz}$. Please note that the results by the adaptive model reported in Figure 2b are obtained directly from constitutive equations, thus confirming the distinctive feature of this structural model, as discussed above. The numerical results confirm the accuracy of the adaptive model here adopted when applied to 3DWC, and therefore they validate the idea of carrying out structural analyses, after having obtained an evaluation of the homogenized mechanical properties of stitched materials.

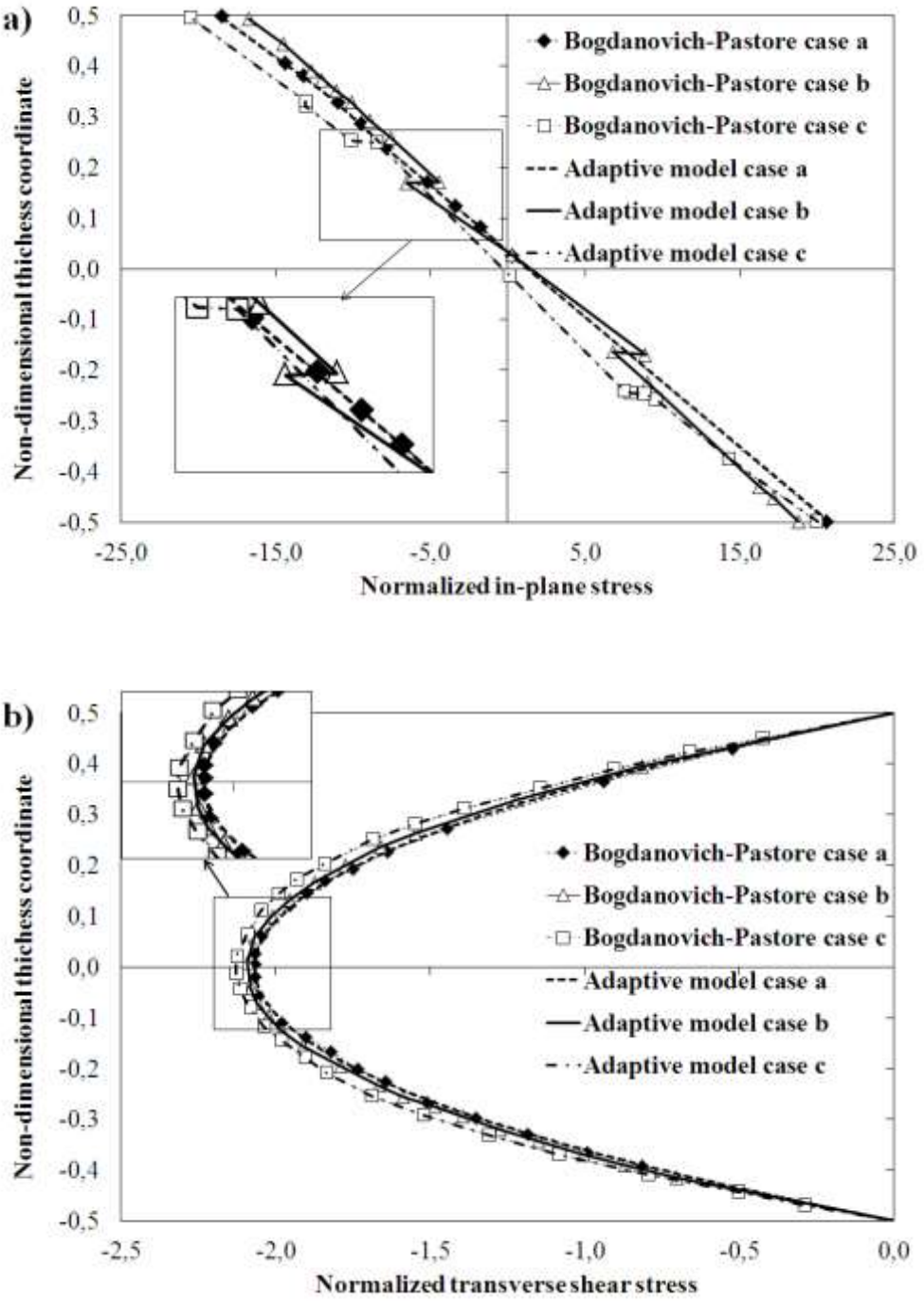

Figure 2. Through-the-thickness distribution of a) in-plane stress $\overline{\sigma}_x$ and b) transverse shear stress $\overline{\sigma}_{xz}$ for the 3D woven composite plate considered by Bogdanovich and Pastore [35].

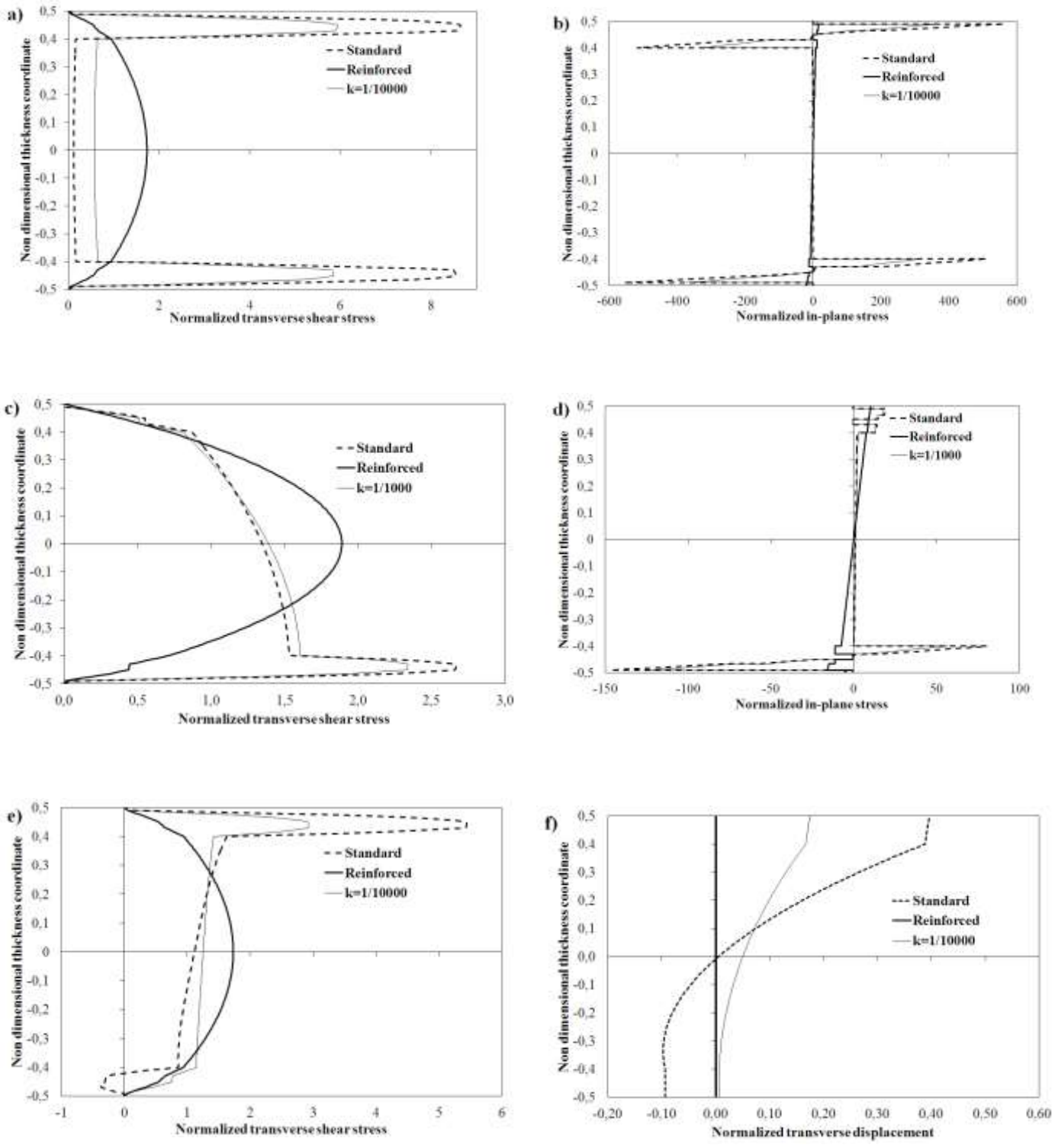

Figure 3. Through-the-thickness distribution of a) transverse shear stress $\overline{\sigma}_{xz}$ and b) in-plane stress $\overline{\sigma}_{x}$ for sandwich beam with damaged core. Through-the-thickness distribution of c) transverse shear stress $\overline{\sigma}_{xz}$ and d)

in-plane stress $\overline{\sigma}_x$ for sandwich beam with damaged upper face (E_1 degraded). Through-the-thickness distribution of d) transverse shear stress $\overline{\sigma}_{xz}$ and e) transverse displacement $\overline{w}$ for sandwich beam with damaged upper face (E_3 degraded).

3.2 Applications to sandwich structures

Applications are presented to three simply supported sandwich beams undergoing sinusoidal loading and then to a square plate with the same boundary conditions and bi-sinusoidal loading. The beams are characterized by a length to thickness ratio of 4, which is quite unrealistic, but it is chosen since it represents a very severe test for the structural model (see, e.g. [30] and [34]). The beams have a (MAT 1/2/3/1/3/4)$_s$ stacking sequence and the following thickness ratios of the constituent layers (0.010/ 0.025/ 0.015/ 0.020/ 0.030/ 0.4)$_s$. Where MAT 1, MAT 2, MAT 3 and MAT 4 have the following properties: MAT 1: E_1=E_3=1 GPa, G_{13}=0.2 GPa, υ_{13}=0.25; MAT 2: E_1=33 GPa, E_3=1 GPa, G_{13}=0.8 GPa, υ_{13}=0.25; MAT 3: E_1=25 GPa, E_3=1 GPa, G_{13}=0.5 GPa, υ_{13}=0.25; MAT 4: E_1=E_3=0.05 GPa, G_{13}=0.0217 GPa, υ_{13}=0.15.

Damaged beams are simulated using the ply-discount theory as in [34]. In particular, three cases are studied: i) the damage of the core, simulated reducing G_{13} of MAT 4 of a 10^{-2} factor, ii) the damage of the upper face of the structures, simulated reducing E_1 of the materials constituting the upper face of a 10^{-2} factor, and iii) the damage of the upper face of the structures, simulated reducing E_3 of the material constituting the upper face and the core of a 10^{-2} factor. This last case is considered like in [26] and [34], because it determines highly unsymmetrical shear distribution and stress concentration of interlaminar shears, thus constituting a severe test for the model. Displacements and stresses are reported normalised in the following form, according to Ref. [34], where the exact solutions for cases i) and iii) have been computed:

$$\overline{\sigma}_{xz} = \frac{\sigma_{xz}(0,z)}{p^0} \quad \overline{w} = \frac{w\left(\frac{L_x}{2},z\right)}{hp^0} \quad \overline{\sigma}_x = \frac{\sigma_x\left(\frac{L_x}{2},z\right)}{p^0} \tag{24}$$

Stress and displacement fields are represented in Figure 3 and 4. In the first case a T300 reinforcement has been considered, while in the latter the reinforcement has parametric properties, namely, different values of the index “k” (see Eq. (22)) are chosen. In both cases the reinforcing thread has circular section with a 2,5 mm diameter, and the reinforcement percentage volume ‘V’ is 0.1. Please note that in Figure 3

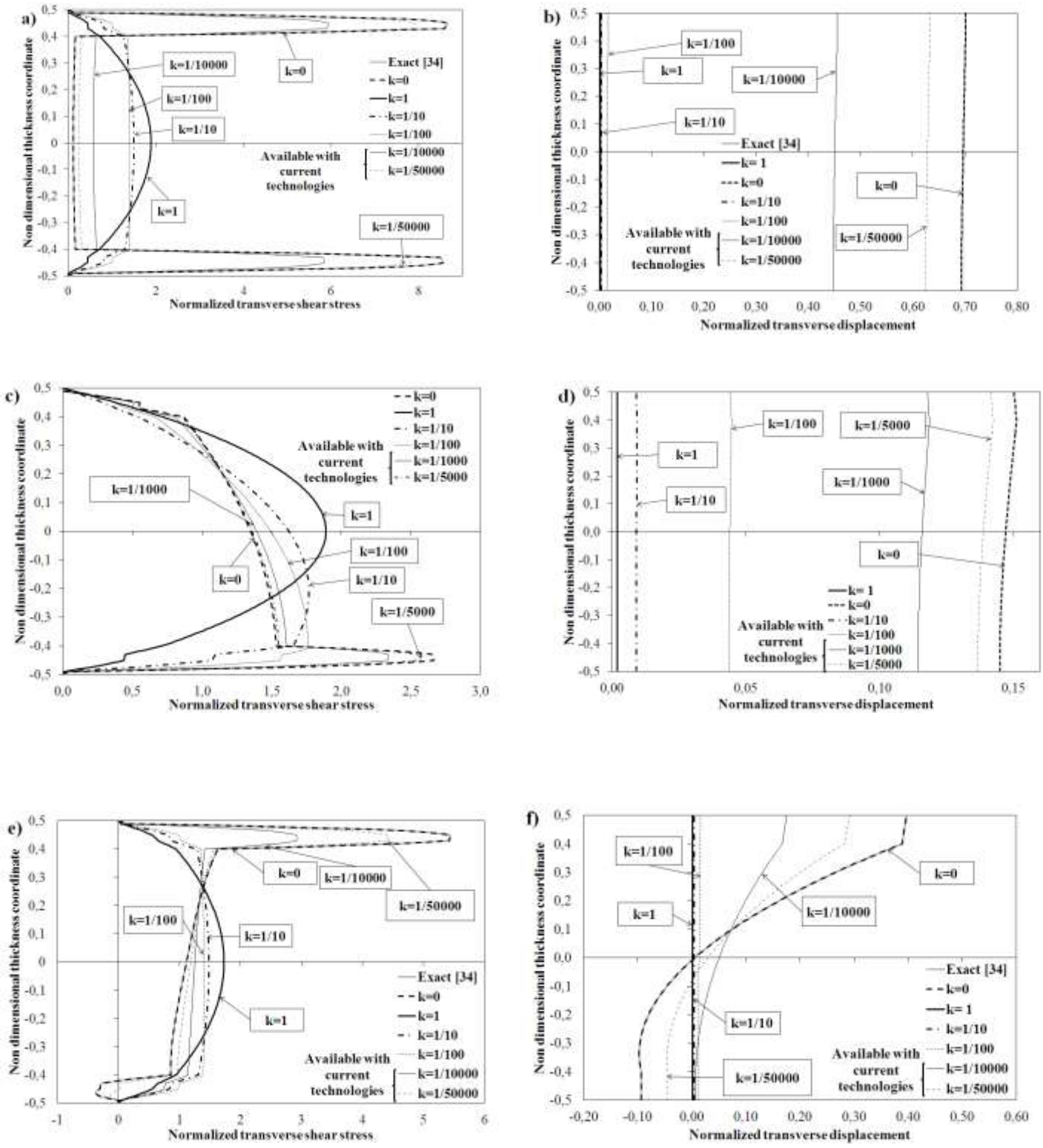

Figure 4. Through-the-thickness distribution of transverse shear stress $\overline{\sigma}_{xz}$ and transverse displacement $\overline{w}$ with parametric properties of the reinforcing thread for: a)-b) sandwich beam with damaged core, c)-d) sandwich beam with damaged upper face (E_1 degraded), d)-e) sandwich beam with damaged upper face (E_3 degraded).

the sandwiches stitched or tufted considering k=1 are named as ‘reinforced’, those with no reinforcement are named as ‘standard’, while in the other cases k is explicitly defined. It could be noticed that the adaptive model provides accurate results directly from constitutive equations, as shown by the comparison with exact elasticity solution (Figs. 4a and 4e). Then, numerical results show that stitching or tufting can be effective ways in reducing the detrimental effects of out-of-plane stresses (Fig. 3a, 3c and 3e) and transverse displacement (Fig. 3f). Stress recovery could be obtained with the insertion of viscoelastic layers (see, e.g. [40]), although at the expense of a consistent stiffness loss.

The last case of analysis considers the sandwich plate examined in Ref. [30], where an accurate stress analysis has been carried out. Our aim is to show whether the beneficial effects of through-the-thickness reinforcement can be obtained also for sandwich plates. The mechanical properties of the Graphite/Epoxy faces are: E_1=132.38 GPa E_2=E_3=10.76 GPa, G_{13}=5.65 GPa, G_{12}=5.62 GPa, G_{23}=3.61 GPa, υ_{12}=υ_{13}=0.24, υ_{23}=0.49; the mechanical properties of the foam core are: E_1= E_2=E_3=0.035 GPa, G_{13}= G_{12}= G_{23}= 0.0123 GPa, υ_{12}=υ_{13}= υ_{23}=0.4. T300 reinforcement with circular section and 2,5 mm diameter and a reinforcement percentage volume ‘V’ of 0.1 have been considered. The plate is square (L_x= L_y= 1 m) and characterized by a length to thickness ratio of 10, with the following thickness ratios of the constituent layers $(0.1/0.4)_s$. Figure 5a represents the through-the-thickness variation of the transverse shear stress σ_{xz}, while Figure 5b represents the through-the-thickness variation of the transverse shear stress σ_{yz}. As in Figure 3 the sandwiches stitched or tufted considering k=1 are named as ‘reinforced’, while those with no reinforcement are named as ‘standard’. From the numerical results of Figure 5 it could be remarked that through-the-thickness reinforcement is effective in reducing the interlaminar shear stresses in sandwich plates.

As general remarks, it could be outlined that stitching determines an increase of transverse shear stresses in the core, and a reduction in the faces. Since experimental results reported in [38]show that stitching through-the-thickness increases the strength of the structure, a great reduction of the delamination index can be obtained. This justifies the experimental results reported in [8] and [14], showing a reduced damage under impact loading.

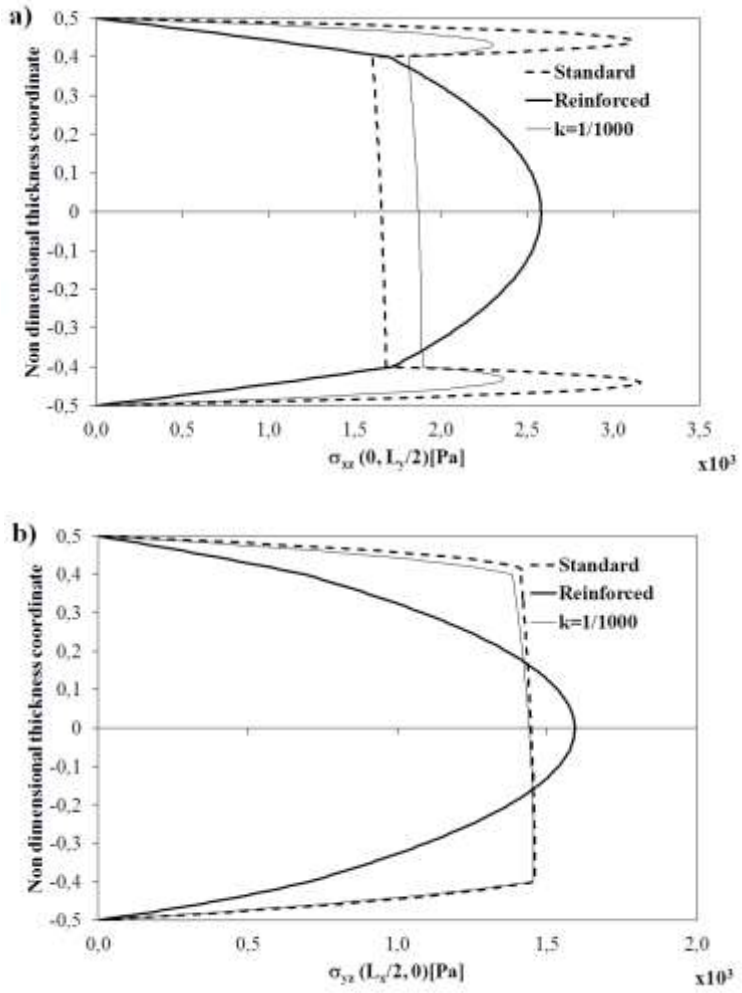

Figure 5. Through-the-thickness distribution of a) transverse shear stress σ_{xz} and b) transverse shear stress σ_{yz} for the square plate.

4 Concluding remarks

An advanced hierarchic model by the authors has been applied to the analysis of stitched or tufted sandwiches, with the purpose of studying the effects of these technical skills on stress and displacements fields. To this aim, we choose to carry out virtual material testing with 3D FEA, in order to get an evaluation of the homogenized mechanical properties of stitched or tufted sandwiches. Then we perform the structural analysis using the adaptive model by the authors. It has a variable representation across the thickness, thus it can adapt itself to the variation of solutions, without an increase in the number of functional d.o.f. These characteristics enable to obtain great accuracy also for the analysis of 3DWC, as shown in the numerical results presented. In fact, they show that the insertion of a reinforcing thread (with

stitching or tufting) in sandwiches considerably reduces the transverse shear stress as well as the transverse displacements.

This behaviour together with the increase of the strength, reported in experimental results taken from literature, should determine a great reduction of the delamination index. This justifies the improved damage tolerance of sandwiches with through-the-thickness subjected to impact loading shown by experiments by other researchers.

References

1. Heimbs S, Cichosz J, Klaus M, Kilchert S, Johnson AF. Sandwich structures with textile-reinforced composite foldcores under impact loads. Comp Struct 2010; 92:1485-1497.

2. De Borst R, Remmers JJC. Computational modelling of delamination. Comp Sci Tech 2006; 66: 713-722.

3. Davies GAO, Hitchings D, Ankersen J. Predicting delamination and debonding in modern aerospace composite structures. Comp Sci Tech 2006; 66: 846-854.

4. Ajdari A, Nayeb-Hashemi H, Vaziri A. Dynamic crushing and energy absorption of regular, irregular and functionally graded cellular structures. Int J of Solids and Struct 2011; 48: 506-516.

5. Gui L, Li Z. Delamination buckling of stitched laminates. Comp Sci Tech 2001; 61(5):629–36.

6. Mouritz AP. Ballistic impact and explosive blast resistance of stitched laminates. Composites: Part B 2001; 32:431–9.

7. Shah Khan MZ, Mouritz AP. Fatigue behaviour of stitched GRP laminates. Comp Sci Tech 1998; 56:695–701.

8. Potluri P, Kusak E, Reddy TY. Novel stitch-bonded sandwich composite structures. Comp Struct 2003; 59:251-259.

9. Judawisastra H, Ivens J, Verpoest I. The fatigue behaviour and damage development of 3D woven sandwich composites. Comp Struct 1998; 43:35-45.

10. Wang B, Wu L, Jin X, Du S, Sun Y, Ma L. Experimental investigation of 3D sandwich structure with core reinforced by composite columns. Materials & Design 2010; 31: 158-165.

11. Vaidya UK, Nelson S, Sinn B, Mathew B. Processing and high strain rate impact response of multifunctional sandwiches composites. Comp Struct 2001; 52: 429-440.

12. Nilanjan M. A methodology for improving shear performance of marine grade sandwich composites: sandwich composite panel with shear key. Comp Struct 2010; 92: 1065-1072.

13. Dow MB, Dexter HB. Development of stitched, braided and woven composite structures in the ACT program and at Langley research center (1985–1997).NASA TP-206234; 1997.

14. Henao A, Carrera M, Miravete A, Castejón L. Mechanical performance of through-thickness tufted sandwich structures. Comp Struct 2010; 92:2052-2059.

15. Prodromou AG, Lomov SV, Verpoest I. The method of cells and the mechanical properties of textile composites. Comp Struct 2001; 93: 1290-1299.

16. Ishikawa T, Chou TW. Stiffness and strength behaviour of woven fabric composites. J Mater Sci 1982; 17:3211–20.

17. Ko FK, Chou TW. Composite materials series – textile structural composites, vol. 3. Amsterdam: Elsevier Science, 1989.

18. Naik NK, Ganesh VK. An analytical method for plain weave fabric composites. Composites 1995; 26:281–9.

19. Ansar M, Xinwei W, Chouwei Z. Modelling strategies of 3D woven composites: a review. Comp Struct 2011; 93:1947–1963.

20. Mori T, Tanaka K. Average stress in matrix and average elastic energy of materials with misfitting inclusions. Acta Metall Mater 1973; 21:571-574.

21. Huysmans G, Verpoest I, Van Houtte P. A poly-inclusion approach for the elastic modelling of knitted fabric composites. Acta Mater 1998; 46: 3003-3013.

22. Eshelby JD. The determination of the elastic field of an ellipsoidal inclusion and related problems. Proc Roy Soc 1957; A241:376–96.

23. Aboudi J. Meso-mechanical analysis of composites by the method of cells. Appl Mech Rev 1989; 42:193–221.

24. Kim SJ, Ji KH, Paik SH. Numerical simulation of mechanical behaviour of composite structures by supercomputing technology. Adv Compos Mater 2008; 17:373–407.

25. Lee CS, Chung SW, Shin H, Kim SJ. Virtual material characterization of 3D orthogonal woven composite materials by large-scale computing. J Compos Mater 2005; 39:851–63.

26. Icardi U, Atzori A. Simple, efficient mixed solid element for accurate analysis of local effects in laminated and sandwich composites. Adv in Eng Soft 2004; 32(2):843-849.

27. Meo M, Vignjevic R, Marengo G. The response of honeycomb sandwich panels under low-velocity impact loading. Int J of Mech Sci 2005; 47: 1301-1325.

28. Castaniè B, Bouvet C, Aminanda Y, Barrau JJ, Thevenet P. Modelling of low-energy/low-velocity impact on Nomex honeycomb sandwich structures with metallic skins. Int J Imp Eng 2008; 35: 620-34.

29. Icardi U, Sola F. Development of an efficient zig-zag model with variable representation of displacement across the thickness. Submitted to J Eng Mech.

30. Plagianakos TS, Saravanos DA. Higher-order layerwise laminate theory for the prediction of interlaminar shear stresses in thick composite and sandwich composite plates. Comp Struct 2009; 87:23–35.

31. Shariyat M. A generalized high-order global-local plate theory for nonlinear bending and buckling analyses of imperfect sandwich plates subjected to thermo-mechanical loads. Comp Struct 2010; 92: 130–43.

32. Elmalich D, Rabinovitch O. A higher-order finite element for dynamic analysis of soft-core sandwich plates. J Sandwich Structures & Materials 2012; 14: 525-555.

33. Icardi U, Ferrero L. Multilayered shell model with variable representation of displacements across the thickness. Composites: Part B 2011*;* 428:18-26.

34. Icardi U. Higher-order zig-zag model for analysis of thick composite beams with inclusion of transverse normal stress and sublaminates approximations. Composites: Part B 2001; 32:343-354.

35. Bogdanovich AE, Pastore CM. Material-smart analysis of textile-reinforced structures. Comp Sci Tech 1996; 56:291–309.

36. Gibson LJ, Ashby MF. Cellular solids. Oxford: Pergamon, 1988.

37. Yudhanto A, Watanabe N, Iwahori Y, Hoshi H. Effect of stitch density on tensile properties and damage mechanism of stitched carbon/epoxy composites. Composites: Part B 2013; 46: 151-165.

38. Lascoup B, Aboura Z, Khellil K, Benzeggagh M. Prediction of out-of-plane behaviour of stitched sandwich structure. Composites: Part B 2012; 43: 2915-2920.

39. Wang P, Lei Y, Yue Z. Experimental and numerical evaluation of flexural properties of stitched foam core sandwich structure. Comp Struct 2013; 100: 243-248.

40. Suzuky K, Kageyama K, Kimpara I, Hotta S. Vibration and damping prediction of laminates with constrained viscoelastic layers. Mech Adv Mater Struct 2003; 10(2): 43–73.